

Correlations in nuclear matterM. Baldo^{1,*} and H. R. Moshfegh^{1,2,†}¹*INFN, Sezione di Catania Via S. Sofia 64, I-95123, Catania, Italy*²*Department of Physics, University of Tehran, P.O.B. 14395-547, Tehran, Iran*

(Received 6 May 2012; revised manuscript received 1 July 2012; published 9 August 2012)

We analyze the nuclear matter correlation properties in terms of the pair correlation function. To this aim we systematically compare the results for the variational method in the lowest-order constrained variational (LOCV) approximation and for the Brueckner-Hartree-Fock (BHF) scheme. A formal link between the Jastrow correlation factor of LOCV and the defect function (DF) of BHF is established and it is shown under which conditions and approximations the two approaches are equivalent. From the numerical comparison it turns out that the two correlation functions are quite close, which indicates in particular that the DF is approximately local and momentum independent. The equations of state (EOS) of nuclear matter in the two approaches are also compared. It is found that once the three-body forces (TBF) are introduced, the two EOS are fairly close, while the agreement between the correlation functions holds with or without TBF.

DOI: [10.1103/PhysRevC.86.024306](https://doi.org/10.1103/PhysRevC.86.024306)

PACS number(s): 21.65.Mn, 26.60.-c, 13.75.Cs, 03.75.Ss

I. INTRODUCTION

The structure and properties of nuclear matter is one of the central issues in the development of nuclear many-body theory. Nuclear matter is of great relevance for the physics of supernova, neutron stars, and heavy ion collisions, for the development of density functionals in nuclear structure studies, and for the understanding at fundamental level of the low-energy baryon-baryon interaction. For a review see Ref. [1]. Different many-body theories [2,3] have been developed to approach this problem. One can mention the variational method [4–11], the Monte-Carlo method in its different versions [12–17], and the diagrammatic expansion methods, in particular the Brueckner-Bethe-Goldstone hole-line expansion [2] and the self-consistent Green's function scheme [18–25]. One of the main goals of this effort along the years has been the explanation of the saturation point of nuclear matter that can be extracted phenomenologically through various experimental methods, in particular the analysis of the binding energy of nuclei and of the electron elastic scattering cross sections [1]. However, besides the saturation point, one of the most important characteristics of nuclear matter is its correlation structure. In fact, the presence of a hard core in the nucleon-nucleon (NN) interaction produces a correlation “hole” between two nucleons that can be described by the correlation function. The latter is also determined by the intermediate and long-range interaction, typical of the nuclear two-nucleon potential. The correlation function is a key quantity to characterize each many-body scheme and to understand the corresponding numerical results. In scattering studies, the spectral function of a many-fermion system gives the important quantities of interest and the short- and long-range correlation functions are very important factors for calculating the spectral functions [26]. The connection of the correlation function and the spectral function is not

straightforward, but it has been elucidated in Ref. [27] in the Brueckner-Hartree-Fock (BHF) framework and in Ref. [28] for the lowest-order constrained variational (LOCV) method, where it is particularly transparent. Furthermore, several phenomena that occur in neutron star matter are closely linked to the correlation function, such as, e.g., dissipation due to shear viscosity and neutrino transport. It appears, then, natural to look for a comparison between the correlation functions from different many-body schemes. In this paper we present a detailed comparison between the Bethe-Brueckner-Goldstone (BBG) method [2] and the variational method, as developed within the LOCV framework. Both methods have been applied systematically to nuclear matter with different two-body interactions. The results for the saturation point and other physical parameters, such as the compressibility at high density [29,30] and the critical temperature of the liquid-gas phase transition [31,32], are close but not completely in agreement. One of the main goals of this work is to present an analysis of the correlation function that could help understanding the reason of the agreements and the discrepancies by the comparison of the corresponding correlation properties.

II. THE VARIATIONAL METHOD

The method of lowest-order constrained variational approach is among the microscopic methods that were developed to calculate the bulk properties of homogeneous nuclear fluids, such as the saturation quantities by using the realistic nucleon-nucleon interaction, i.e., Reid68 and Δ -Reid (the modified Reid potential with inclusion of isobar degrees of freedom) [33]. This method was reformulated to include more sophisticated interactions [34], such as UV_{14} , AV_{18} [35], and charge-dependent Reid potential (Reid93) [36]. The LOCV method has been also developed for calculating the various thermodynamic properties of hot and frozen homogeneous fermionic fluids, such as symmetric and asymmetric nuclear matter [37], β -stable matter [38], helium-3 [39], and electron fluid [40], with different realistic interactions. Recently, the

*baldo@ct.infn.it

†hmoshfeqh@ut.ac.ir

LOCV formalism was developed for covering the relativistic Hamiltonian with a potential that has been fitted relativistically to nucleon-nucleon phase shifts [41]. The LOCV calculation is a fully self-consistent technique with state-dependent correlation functions. There is no free parameter in this method, except those included in the interactions. Considering constraint, as in the form of normalization condition, is another advantage of LOCV formalism. This assumption keeps the higher-order terms as small as possible, and it also assumes a particular form for the long-range behavior of the correlation functions in order to perform an exact functional minimization of the two-body energy with respect to the short-range parts of correlation functions. The functional minimization procedure represents an enormous computational simplification over the unconstrained methods, where the short-range behavior of the correlation functions is parametrized, which attempt to go beyond the lowest order [42]. To test the convergence of the LOCV method for nuclear matter and helium-3, the calculations were performed beyond the lowest order, and the three-body cluster energy was evaluated with both the state-averaged and state-dependent correlation functions [43]. The smallness of the normalization (the convergence parameter) and of the three-body cluster energy indicated that at least up to twice the empirical nuclear matter saturation density, the cluster expansion converges reasonably, and stopping after two-body cluster terms is a fair approximation. In the LOCV method, we use an ideal Fermi gas-type wave function, ϕ_i , for the single-particle states, and we employ the variational techniques to find the wave function of the interacting system (Refs. [33–36]), i.e.,

$$\Psi = F \Phi, \quad (1)$$

where Φ is the uncorrelated Fermi system wave function (Slater determinant of plane waves) and the factor $F(1, 2, \dots, A)$ is the many-body correlation function, defined as a product of two-body correlation functions $f(i, j)$ (Jastrow form), and assumes that they are operators,

$$F = \mathcal{S} \prod_{i < j} f(i, j), \quad (2)$$

where \mathcal{S} is a symmetrizing operator. The many-body energy term $E[f]$, which is a functional of the f 's, is calculated by constructing a cluster expansion for the expectation value of Hamiltonian H of the system:

$$E[f] = \frac{1}{A} \frac{\langle \Psi | H | \Psi \rangle}{\langle \Psi | \Psi \rangle} = E_1 + E_2 + \dots \dots \dots > E_0, \quad (3)$$

where E_0 is the true ground-state energy and A is the particle number. In the lowest order we truncate the above series after E_2 , i.e., two-body energy. The one body term E_1 is independent of the f and is just the familiar Fermi gas kinetic energy. The two-body energy term is defined as

$$E_2 = \frac{1}{2A} \sum_{ij} \langle ij | W | ij \rangle_a; \quad |ij\rangle_a = |ij\rangle - |ji\rangle \quad (4)$$

$$W = -\frac{\hbar^2}{2m} [f(1, 2), [\nabla^2, f(1, 2)]] + f(1, 2)V(1, 2)f(1, 2),$$

and the two-body antisymmetrized matrix element $\langle ij | W | ij \rangle_a$ is taken with respect to the single-particle functions composing ϕ_i , i.e., plane-waves. By inserting a complete set of two-particle states twice in the above equation and performing some algebra, we can rewrite the two-body term as a functional of correlation functions [33,34,36]. In this equation, $V(1, 2)$ is a phenomenological nucleon-nucleon potential such as Reid type, UV_{14} , and AV_{18} . At this stage, we can minimize the two-body energy with respect to the variations of the correlation functions [33,34,36] but subject to the normalization constraint [33–41]:

$$\frac{1}{A} \langle ij | h^2(1, 2) - f^2(1, 2) | ij \rangle_a = 1. \quad (5)$$

The function $h(1, 2)$ is the modified Pauli function, which for the symmetrical nuclear matter takes the following form:

$$h(1, 2) = \left\{ 1 - \frac{9}{4} \left[\frac{j_1(r_{12})}{r_{12}} \right]^2 \right\}^{-\frac{1}{2}}, \quad (6)$$

where $j_1(r_{12})$ is the well-known spherical Bessel function of order 1. Note that $[\chi = \langle \Psi | \Psi \rangle - 1]$ plays the role of a smallness parameter in the cluster expansion. The above constraint introduces a Lagrange multiplier, through which all the correlation functions are coupled. Then we can write sets of uncoupled and coupled Euler-Lagrange differential equations with respect to the correlation functions. The constraint is incorporated by solving these Euler-Lagrange equations only up to a certain distance, where the logarithmic derivative of correlation functions matches those of the Pauli function, and then we set the correlation functions equal to the Pauli function. As we pointed out before, there is no free parameter in our LOCV formalism, i.e., the healing distance is determined directly by the constraint and the initial conditions.

III. THE BBG EXPANSION

One of the most known and used microscopic many-body approaches to the theory of nuclear matter is the Bethe-Brueckner-Goldstone (BBG) expansion [2]. In this scheme, the original nucleon-nucleon interaction is systematically replaced by the so-called G matrix, which describes the two-nucleon scattering amplitude inside the medium. A modified perturbative expansion is then developed in terms of this effective interaction and the different terms can be represented by diagrams. The G matrix can be defined also for singular interaction, e.g., with a hard core, and it is expected to be “smaller” than the original NN interaction. Although all modern realistic NN interactions introduce a finite repulsive core, it is, however, quite large, and therefore in any case a straightforward perturbative expansion cannot be applied. As discussed in the presentation of the variational method, the repulsive core is expected to modify strongly the ground-state wave function whenever the coordinates of two particles approach each other at a separation distance smaller than the core radius c . In such a situation the wave function should be sharply decreasing with the two-particle distance. The “wave function” of two particles in the unperturbed ground state ϕ_0

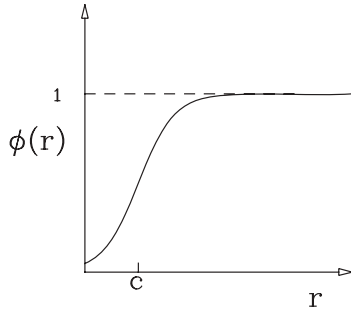


FIG. 1. Schematic representation of the expected effect of the core repulsion on the two-body wave function in nuclear matter.

can be defined as ($k_1, k_2 \leq k_F$)

$$\begin{aligned} \phi(r_1, r_2) &= \langle \phi_0 | \psi_{\xi_1}^\dagger(\mathbf{r}_1) \psi_{\xi_2}^\dagger(\mathbf{r}_2) a_{k_1} a_{k_2} | \phi_0 \rangle \\ &= e^{i(\mathbf{k}_1 + \mathbf{k}_2) \cdot \mathbf{R}} e^{i(\mathbf{k}_1 - \mathbf{k}_2) \cdot \mathbf{r}/2}, \end{aligned} \quad (7)$$

where $\xi_1 \neq \xi_2$ are spin-isospin variables, and $\mathbf{R} = (\mathbf{r}_1 + \mathbf{r}_2)/2$, $\mathbf{r} = (\mathbf{r}_1 - \mathbf{r}_2)$ are the center of mass and relative coordinate of the two particles, respectively. Therefore, the wave function of the relative motion in the s wave is proportional to the spherical Bessel function of order zero $j_0(kr)$, with k the modulus of the relative momentum vector $\mathbf{k} = (\mathbf{k}_1 - \mathbf{k}_2)/2$. The core repulsion is expected to act mainly in the s wave, since it is short range, and therefore this behavior must be strongly modified. In the simple case of $k = 0$, the free wave function $j_0(kr) \rightarrow 1$, and schematically one can expect a modification, due to the core, as depicted in Fig. 1.

The main effect of the core is to “deplete” the wave function close to $r = 0$, in a region of the order of the core radius c . Of course, the attractive part of the interaction will modify this simple picture at $r > c$. If the core interaction is the strongest one, then the average probability p for two particles to be at distance $r < c$ would be a measure of the overall strength of the interaction. If p is small, then one can try to expand the total energy shift ΔE due to the interaction in power of p . The power p^n has, in fact, the meaning of probability for n particles to be all at a relative distance less than c . In a very rough estimate, p is given by the ratio between the volume occupied by the core and the average available volume per particle

$$p \approx \left(\frac{c}{d} \right)^3, \quad (8)$$

with $\frac{4\pi}{3}d^3 = \rho^{-1}$. From Eq. (8) one gets $p \approx \frac{8}{9\pi}(k_F c)^3$, which is small at saturation, $k_F = 1.36 \text{ fm}^{-1}$, and the commonly adopted value for the core is $c = 0.4 \text{ fm}$. The parameter remains small up to a few times the saturation density.

The terms of the expansion can now be ordered according to the order of the correlations they describe, i.e., the power in p they are associated with. It is easy to recognize that this is physically equivalent to grouping the diagrams according to the number of hole lines they contain, where n -hole lines correspond to n -body correlations. In fact, an irreducible diagram with n -hole lines describes a process in which n particles are excited from the Fermi sea and scatter in some way above the Fermi sea. Equivalently, all the diagrams with n -hole lines describe the effect of clusters of n particles, and

therefore the arrangement of the expansion for increasing number of hole lines is called alternatively “hole expansion” or “cluster expansion.” For a pedagogical introduction to the BBG expansion, see Refs. [2,44], where references to more technical reviews can be found. In Ref. [44] the connection of BBG and the variational method is discussed. The relation between the two approaches turns out to be more transparent if the BBG expansion is reformulated in terms of the coupled cluster method (or e^S method) [45]. According to this scheme, the wave function of the ground state is written

$$|\Psi\rangle = e^{\hat{S}}|\Phi\rangle, \quad (9)$$

where \hat{S} is a correlation operator containing a set of n -body terms, which produce excitations of n particles from below to above the Fermi sea. This method has also a variational character, in the sense that the variation is performed not on the ground-state wave function but on these correlation terms [45,46]. Then a set of coupled equations is obtained for the n -body correlation functions. The expansion of this set of equations in terms of the order of the correlations is equivalent to a reordering of the hole-line expansion in the BBG theory [47]. At the two-body level of approximation, the method is equivalent to the so-called Brueckner approximation [44,47] in the BBG hole-line expansion, and the operator \hat{S} reduces to a two-body operator \hat{S}_2

$$\hat{S}_2 = \sum_{k_1 k_2, k'_1 k'_2} \langle k'_1 k'_2 | S_2 | k_1 k_2 \rangle a^\dagger(k'_1) a^\dagger(k'_2) a(k_2) a(k_1), \quad (10)$$

where the k 's label hole state, i.e., inside the Fermi sphere, and the k' 's particle states, i.e., outside the Fermi sphere. Each quantity k indicates momentum \mathbf{k} and spin-isospin quantum numbers. The function \hat{S}_2 is the so called “defect function” of the Brueckner scheme. It can be written in terms of the G matrix and it is just the difference between the in-medium interacting and noninteracting two-body wave functions [2,44]. The different terms of the summation commute with each other and expanding the exponential in Eq. (9) one gets the product of the correlation operators over all sets of momenta,

$$\begin{aligned} |\Psi\rangle &= \prod_{\{k\}} \left[1 + \sum_{k'_1 k'_2} \langle k'_1 k'_2 | S_2 | k_1 k_2 \rangle a^\dagger(k'_1) \right. \\ &\quad \left. \times a^\dagger(k'_2) a(k_2) a(k_1) \right] |\Phi\rangle, \end{aligned} \quad (11)$$

where the product is over all disjoint pairs of momenta k_1, k_2 , in a given partition of the set of all momenta, in agreement with the Brueckner scheme, which is an independent pair approximation. Higher orders in the expansion vanish because they include powers of annihilation or creation operators. In the square bracket one can recognize the two-body wave function. After Fourier transformation to coordinate representation and assuming the defect function to be local and independent of total momentum, this expression acquires the same form as in the variational method, where the two-body wave function plays the role of the correlation factors $f(i, j)$. However, there are relevant differences with the variational method. First of all the BBG expansion is not explicitly variational,

although, as already mentioned, one can recast the expansion in terms of the e^S scheme, which can be formulated by means of a particular variational procedure [44,45]. Second, the G matrix, and therefore the defect function, is in general highly nonlocal, which means that the two-body wave function is dependent also on the initial momenta in the Fermi sea, as well as on the total momentum. This would imply a correlation factor in integral form for the variational scheme. Furthermore, in BBG expansion one introduces a single particle auxiliary potential, in order to increase the degree of convergence of the expansion. This potential is usually called Brueckner potential and it is determined with a self-consistent procedure [2]. In the variational method, no single-particle potential is introduced in the minimization procedure. Of course, it is hidden in the mean value of the Hamiltonian, but it can be calculated only after the optimal many-body wave function and energy have been obtained, by adding a tiny fraction of particle to the system [48]. Finally, in the variational method the correlation function is introduced in the mean value of both the kinetic energy and the interaction term. It is a peculiarity of the BBG expansion that the total energy is written as the sum of the unperturbed kinetic energy and the correlated interaction energy. The latter includes, of course, implicitly the effect of the correlation on the kinetic energy due to the momentum dependence of the single particle potential and of the G matrix.

It is one of the main purposes of this work to explore the consequences of these differences on the correlation properties of the ground state. In turn, the study provides a detailed view of the nuclear matter correlations. Since for both LOCV and the BBG expansion three-body correlations turns out to be only a fraction of MeV around saturation density [44,49,50], we restrict the comparison to two-body correlations. In any case, the two-body correlation functions are determined at the BHF level for the BBG expansion and at the two-body Jastrow-like factors for the variational method.

IV. FORMAL AND NUMERICAL COMPARISON

In order to formulate a meaningful comparison between the two-body microscopic methods, we introduce a mixed representation of the correlation functions. In the expansion of Eq. (11) we separate relative and total momenta and perform the Fourier transformation on the momenta k' , i.e., the final ones above the Fermi sea. One gets in this way the correlation function F in coordinate representation, which is dependent on the initial relative momentum and on the total momentum

$$\int \frac{d^3q'}{(2\pi)^3} e^{iq'r} [\delta_{qq'} + \langle q' | S_2(P) | q \rangle] = F_B(r; q, P), \quad (12)$$

where the defect function can be written in terms of the G matrix,

$$\langle q' | S_2(P) | q \rangle = \frac{Q(q', P)}{e(q', q, P)} \langle q' | G(P) | q \rangle, \quad (13)$$

where Q is the average Pauli operator and e is the average two-particle excitation energy; see the Appendix for more details. Because of this averaging, the denominator in Eq. (13) can vanish. The integral of Eq. (12) is meant as principal value,

in agreement with the BHF calculations of the nuclear matter EOS.

The correlation function can be expanded in partial waves and one can define a correlation function for each two-body channel, identified by the quantum numbers $LSJT$ of the relative angular momentum, total spin, total angular momentum, and total isospin, respectively. As shown in the Appendix, the correlation function F_B has to be compared with the corresponding correlation function F_V for the variational method

$$F_V(r, q) = f(r) \times j_l(qr), \quad (14)$$

where j_l is the spherical Bessel function of order l and $f(r)$ is the correlation function of, e.g., Eq. (5). It is essential to notice the factorization of the free wave function characteristic of the variational method. For the Brueckner correlation function F_B this property does not hold, which embodies the nonlocality of the G matrix. However, it can hold approximately, and this can be verified by, e.g., the numerical comparison between the two correlation functions. Details on the formal comparison between F_V and F_B can be found in the Appendix.

We consider symmetric nuclear matter around saturation and we take the potential Argonne v_{18} [35] as the two-body nucleon-nucleon interaction. At the Fermi momentum $k_F = 1.36 \text{ fm}^{-1}$, corresponding to density 0.17 fm^{-3} , we compare in Fig. 2 the correlation functions $F_V(r)$ and $F_B(r)$ at the relative initial momentum $q = 0.1 \text{ fm}^{-1}$ and at zero total momentum P . In this case the correlation functions are calculated for the 1S_0 channel. In the variational method a small hard core of radius $R_c = 0.1 \text{ fm}$ is introduced for numerical reasons, which is apparent from the figure since the correlation function F_V is zero below the core radius. Both correlation functions feel in any case the repulsive, but finite, core of the interaction and they decrease sharply at short distance. They agree closely above the small core radius R_c . At large distances both correlation functions reach the expected value of 1, but just above the repulsive core they exceed 1, due to the attractive part of the NN interaction. In this region they practically coincide.

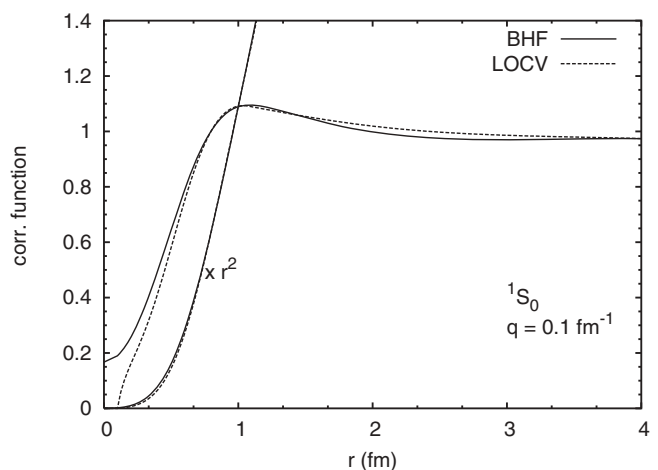


FIG. 2. Correlation function in the 1S_0 channel for the LOCV and BHF approaches. The same correlation functions multiplied by r^2 are also shown. The momentum $q = 0.1 \text{ fm}^{-1}$ is the relative momentum of the two correlated particles.

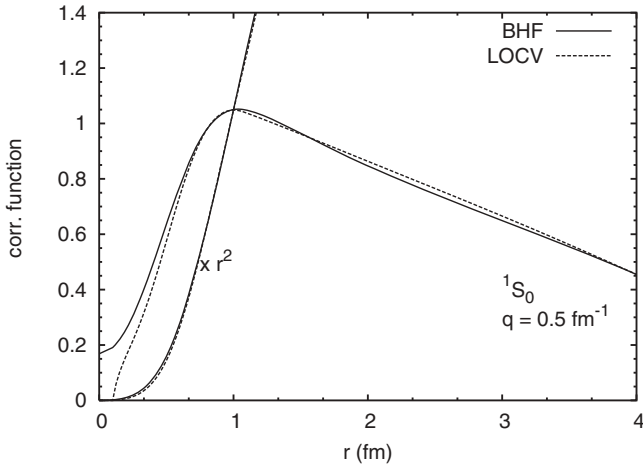


FIG. 3. The same as described in the legend of Fig. 2 but for $q = 0.5 \text{ fm}^{-1}$.

A small discrepancy is observed at intermediate distances, where F_V is slightly larger than F_B . To be more quantitative, we calculated the mean absolute deviation for $r > 0.25 \text{ fm}$. We found a value below 2%, as in all cases we are going to consider in the following.

The comparison for the 1S_0 channel, but for $q = 0.5 \text{ fm}^{-1}$, is reported in Fig. 3. In this case already at moderate distance the two-body wave function F starts to oscillate since it smoothly merges into the free wave function, i.e., the Bessel function (of order 0 in this case). The same agreement between F_V and F_B is observed. This result indicates that the factorization of Eq. (14) is approximately valid also for the correlation function F_B of the BBG expansion. It is also an indication that the defect function is approximately local.

Notice that in the numerical calculations the correlation functions are multiplied by r^2 and therefore the contribution of the small distances is vanishing small. This is illustrated in the same figures, where the correlation functions multiplied by r^2 are reported. In this case the very close agreement is apparent. A similar trend is obtained for the 3S_1 channel; see

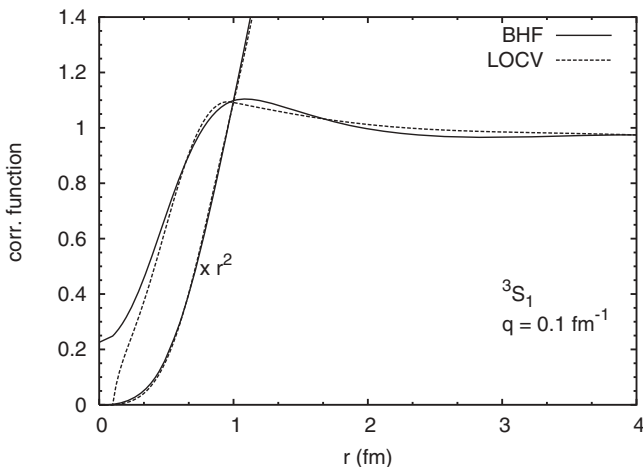


FIG. 4. The same as described in the legend of Fig. 2 but for the 3S_1 channel.

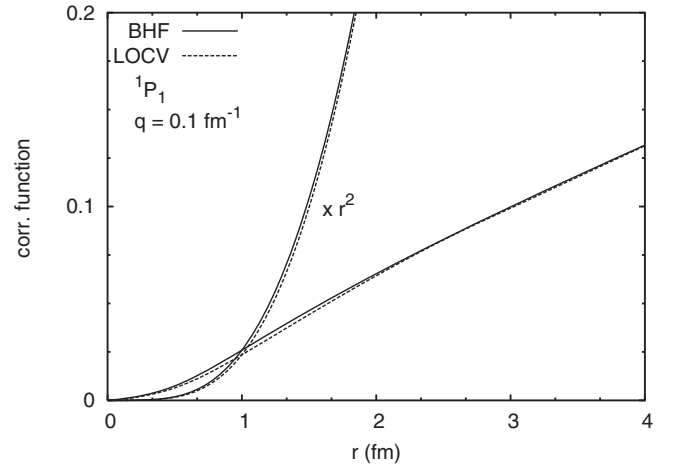


FIG. 5. The same as described in the legend of Fig. 2 but for the 1P_1 channel.

Fig. 4. In the channels with higher partial waves the agreement is even better. To put in evidence the tiny differences, we have reported in an amplified scale the correlation functions in Fig. 5 for the 1P_1 channel and in Fig. 6 for the 3P_1 channel. Notice the change of scale with respect to the previous figures. In these cases the centrifugal barrier suppresses further the two-body wave functions at short and intermediate distance. At larger distance, outside the considered range, the correlation functions merge into the proper Bessel function and then they obviously coincide.

We also checked the dependence on the total momentum that is present in the two-body wave function. It turns out that this dependence is quite weak (see Fig. 7), which justifies the assumption, intrinsic in the variational method, of neglecting such a dependence. Finally, we have introduced the three-body forces (TBF) in the calculations, both in the LOCV and the BBG schemes. It is well known that TBF are necessary if the phenomenological saturation point of nuclear matter has to be reproduced. At the level of two-body correlation approximation, as BHF and LOCV, the TBF are reduced to an

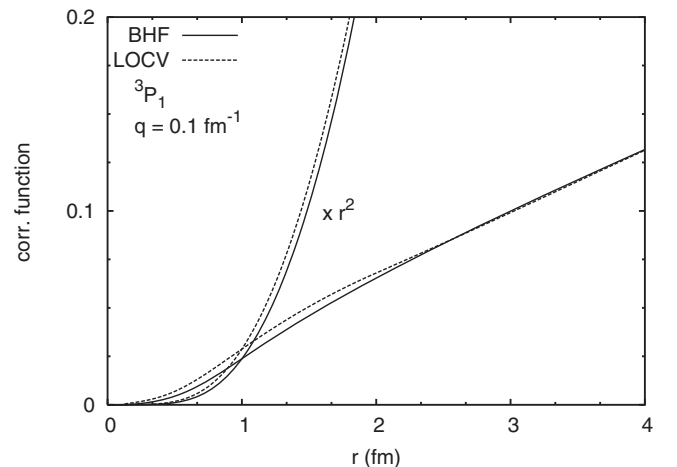


FIG. 6. The same as described in the legend of Fig. 2 but for the 3P_1 channel.

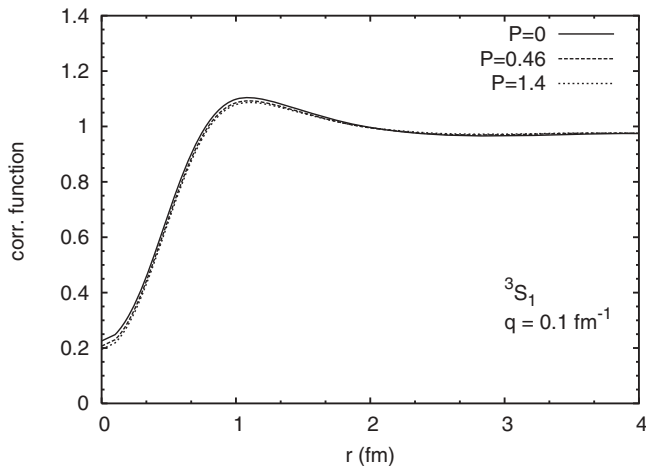


FIG. 7. The correlation functions as in Fig. 4 at different total momentum P of the two correlated particles.

effective two-body force by averaging on the position and on spin-isospin of the third particle [51]. The averaging involves the two-body correlation itself. In principle the original TBF can be derived within the nucleon-meson model of nuclear

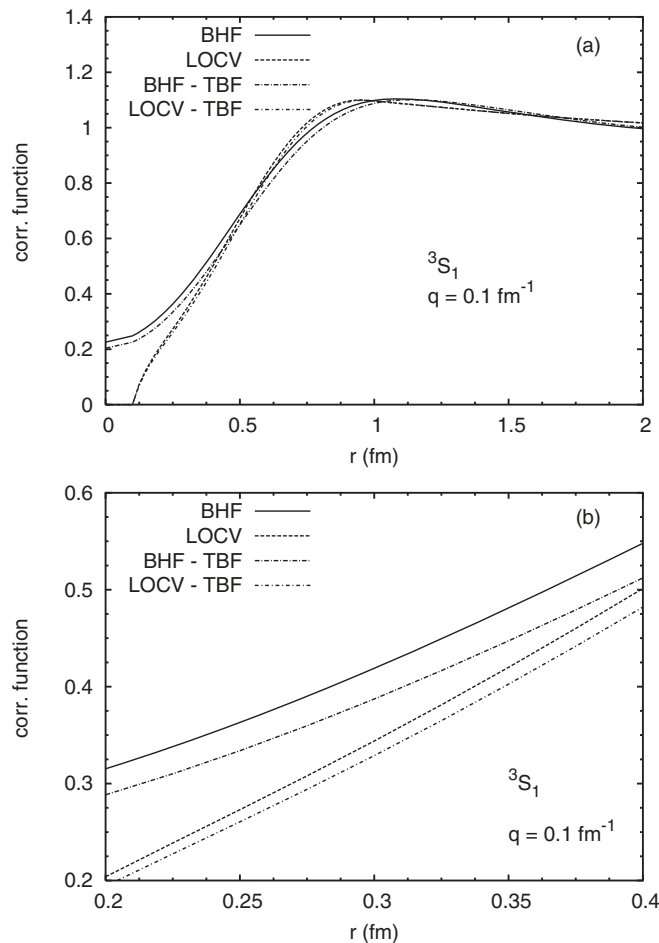


FIG. 8. (a) The correlation function in the 3S_1 channel is reported, with and without three-body forces. (b) The blow up of the plot in (a) within a region at small distances.

forces. This procedure turns out to have only a limited success [52,53] and requires in any case the tuning of the parameters (masses and coupling constants) to get a reasonable saturation point. The latter can be obtained only with the Bonn B potential [54,55] as two-body forces [52,53]. We prefer to follow a more pragmatic point of view. We used the Urbana IX model and treated the TBF according to the method adopted in Ref. [31], where the averaging is performed by using a schematic two-body correlation function. We then tune the (two) parameters of the TBF to get a good saturation point for BHF and we use the same values in LOCV. Around saturation the contribution of TBF is relatively small in absolute value, about 1–3 MeV, in comparison with the total correlation energy that is about -40 MeV at this density. It is slightly repulsive, and as a consequence the two-body wave function is further reduced. This is illustrated in Fig. 8. Since the effect is quite small, as expected by the relatively weakness of the TBF, Fig. 8(b) shows a blow up of the small distance region. It looks as if the effect of the TBF is slightly larger for the BHF method.

V. DISCUSSION AND CONCLUSION

We have studied the correlation properties of nuclear matter both in the variational LOCV method and in the BHF scheme. In particular we have shown that one can identify the variational (generalized) Jastrow factor $F_V(r)$ with the BHF correlation function $F_B(r) = 1 + g(r)$, where $g(r)$ is the so-called defect function. Despite the additional total and relative momentum dependence of F_B , not present in F_V , and the different method of approximation, it turns out that the two correlation functions are quantitatively quite similar. This is true for each two-body channel, with or without the inclusion of the three-body forces. To see the possible relation of the small differences between the LOCV and BHF correlation functions to other nuclear matter properties, we have computed the nuclear matter EOS in the two theoretical schemes. The results are reported in Fig. 9. The two lower curves, labeled 2BF, correspond to the EOS with two-body forces only, while the two upper curves, labeled 2BF + 3BF, correspond to the EOS when the (same) three-body forces are also included. One can notice that the two EOS are much more similar when the three-body forces are included. This is in line with the similar finding [56] that the EOS's with different NN interactions become much closer when the (same) three-body force is included.

In the variational method the average kinetic energy is affected directly by correlations. The total correlation energy includes a kinetic energy part and a potential part; see Eq. (4). The breakdown of the two contributions as a function of density is reported in Table I for the case where TBF are included. For comparison the total potential energy of the BHF calculations is also reported. In the BHF scheme the kinetic energy is not explicitly modified [2], and the whole correlation energy is contained in the potential energy coming from the G matrix contribution. The modification of the kinetic energy is embodied in the momentum dependence of the G matrix and in the self-consistent single-particle potential, which also affects the total binding indirectly since it determines the entry energy of the G matrix. From the results it looks as if the connection

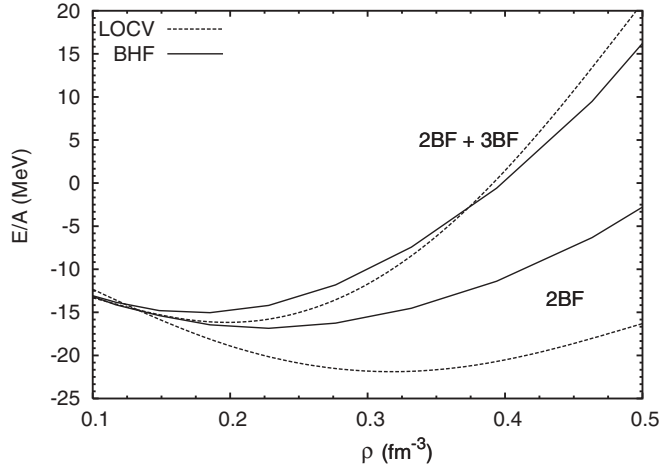


FIG. 9. Binding energy per particle as a function of the density ρ in symmetric nuclear matter for the LOCV and BHF approaches. The two lower curves, labeled 2BF, correspond to calculations with two-body force only. The two upper curves, labeled 2BF + 3BF, correspond to calculations with the inclusion of the three-body forces.

of the EOS and the details of the correlation function is not so straightforward. This is apparent if we calculate the correlations functions at twice the saturation density. They are displayed in Fig. 10(a) for the case with only two-body forces. The agreement between the two correlations looks insensitive to the introduction of the TBF [see Fig. 10(b)] and indeed quantitatively the disagreement, as anticipated before, is below 2% for $r > 0.25$ fm, with or without TBF. Despite the fact that small variations can be relevant, it looks unlikely that this deviation can be considered responsible for the fact that the disagreement between BHF and LOCV is reduced by several MeV at this density once TBF are introduced. It has to be noticed that in BHF there is no simple way to relate the binding energy to the correlation function, which is not directly involved in the BHF expression for the correlation energy. The change of the binding is clearly due to the direct effect of the change in the nucleon-nucleon force due to the TBF. The only effect of TBF on the correlation function [see Fig. 10(b)] seems to be a very small decrease at intermediate distance

TABLE I. Nuclear matter correlation energy per particle in LOCV and in BHF as a function of the density ρ . The first column (K.E.) for LOCV gives the modification of the kinetic energy due to the two-body correlation, the second one (P.E.) the potential part, and the third one their sum. For comparison, the BHF total correlation energy is reported in the last column. The three-body forces are included.

$\rho(\text{fm}^{-3})$	LOCV			BHF
	K.E.	P.E.	TOT	
0.10	11.24	-40.75	-29.51	-29.24
0.17	16.77	-56.09	-39.32	-37.97
0.20	18.94	-61.20	-42.26	-40.42
0.30	25.62	-71.18	-45.56	-43.60
0.34	28.20	-72.34	-44.14	-43.10
0.40	32.12	-71.83	-39.71	-40.46
0.50	36.68	-64.32	-27.64	-31.07

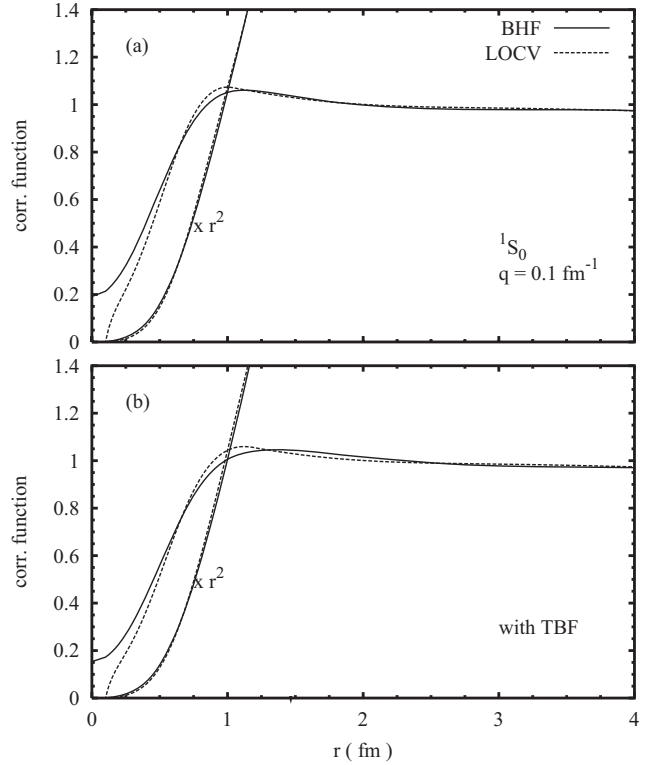


FIG. 10. Correlation function in the 1S_0 channel for the LOCV and BHF approaches at the density $\rho = 0.32 \text{ fm}^{-3}$. The same correlation functions multiplied by r^2 are also shown. The momentum $q = 0.1 \text{ fm}^{-1}$ is the relative momentum of the two correlated particles. (a) Only two-body forces. (b) Three-body forces are included.

of F_V with respect to F_B . This could suggest that the good agreement of the EOS is the result of a redistribution of the attractive and the repulsive contributions to binding. To make easier the qualitative estimate of the relevance of the TBF, we have reported in Fig. 11 the comparison of the correlation

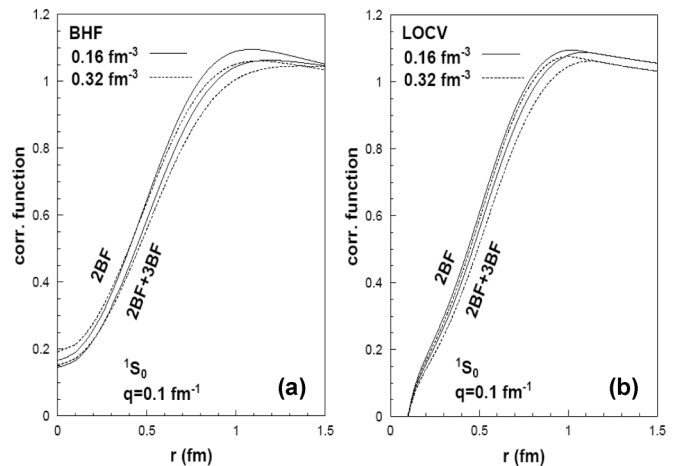


FIG. 11. Comparison of the effect of the TBF on the correlation function at two different densities, 0.16 fm^{-3} (full lines) and 0.32 fm^{-3} (dashed lines). At each density the lower curves include the TBF. Panel (a) refers to BHF; panel (b) refers to LOCV. The meaning of the other labels is as in previous figures.

functions with and without TBF at the densities 0.16 fm^{-3} and 0.32 fm^{-3} , both for LOCV and BHF. At increasing density the effect of TBF increases, but the effect looks larger for BHF. Also in this case no systematic trend is observed in relation to the corresponding EOS. It has been found in Ref. [57] that also the spectral function has a mild dependence on the presence of TBF. Beside the EOS, other quantities, such as transport coefficients or neutrino and electron scattering cross sections, are probably more directly related to the correlation and spectral function [58]. The analysis of this point is left to a future work, but in any case no major discrepancy can be expected between BHF and LOCV schemes.

ACKNOWLEDGMENTS

H.R.M. thanks the University of Tehran for partially supporting him under the grants provided by the research council. This work was supported by INFN Sezione di Catania under national Project No. CT51.

APPENDIX

In this Appendix we give some details on the formal comparison between the effective correlation factor F_B that is present in the ground-state wave function of the Brueckner approximation, within the BBG hole-line expansion, and the corresponding correlation factor F_V in the variational LOCV approximation. The unperturbed ground-state Φ is the antisymmetrized product of N single-particle momentum states

$$|\Phi\rangle = \Pi_{k_i} a_{k_i}^\dagger |O\rangle, \quad (\text{A1})$$

where $|O\rangle$ is the vacuum state and the k_i include spin-isospin variables. Then, Eq. (11) can be rewritten as

$$|\Psi\rangle = \Pi_{\{k_1 k_2\}} \hat{F}_{k_1, k_2} |O\rangle \quad (\text{A2})$$

$$\hat{F}_{k_1 k_2} = \sum_{k'_1 k'_2} [\delta_{k'_1 k_1} \delta_{k'_2 k_2} + \langle k'_1 k'_2 | Q S_2 | k_1 k_2 \rangle] a^\dagger(k'_1) a^\dagger(k'_2),$$

where the summations in \hat{F} are over all momenta and we have introduced the Pauli operator Q that restricts the momenta $k'_1 k'_2$ outside the Fermi sphere, while the momenta $k_1 k_2$ are inside the Fermi sphere.

It is convenient to introduce the wave function of the correlated ground-state $|\Psi\rangle$ by taking the scalar product with

the antisymmetrized N -particle coordinate states

$$|r_1 r_2 \dots r_N\rangle = \Pi_i \psi^\dagger(r_i) |O\rangle = |\{r_i\}\rangle, \quad (\text{A3})$$

where $\psi^\dagger(r_i)$ is the creation operator of a particle at the position r_i (including spin-isospin variables). One gets

$$\Psi(\{r_i\}) = \langle \{r_i\} | \Psi \rangle = A_{\{r_i\}} \Pi_{\{k_1 k_2\}} f_{k_1 k_2}(r_i, r_j), \quad (\text{A4})$$

where the operator A antisymmetrizes the N coordinates r_i and

$$f_{k_1 k_2}(r_i, r_j) = \sum_{k'_1 k'_2} [\delta_{k'_1 k_1} \delta_{k'_2 k_2} + \langle k'_1 k'_2 | Q S_2 | k_1 k_2 \rangle] \times \langle r_i | k'_1 \rangle \langle r_j | k'_2 \rangle, \quad (\text{A5})$$

which is the Fourier transform of the defect function. The variables r_i and r_j are two generic coordinates among the N antisymmetrized ones. Introducing the coordinate representation for the defect function, one gets

$$f_{k_1 k_2}(r_i, r_j) = \langle r_i | k_1 \rangle \langle r_j | k_2 \rangle + \langle r_i r_j | Q S_2 | k_1 k_2 \rangle$$

$$= \langle r_i | k_1 \rangle \langle r_j | k_2 \rangle + \int d^3 r'_i d^3 r'_j \langle r_i r_j | Q S_2 | r'_i r'_j \rangle \times \langle r'_i | k_1 \rangle \langle r'_j | k_2 \rangle. \quad (\text{A6})$$

We consider the relative coordinate $r_{ij} = (r_i - r_j)$ and center of mass coordinate $R_{ij} = (r_i + r_j)/2$ and notice that the defect function $Q S_2$ is diagonal in the total momentum P . If, furthermore, we assume that the defect function is local, one gets

$$f_{k_1 k_2}(r_i, r_j) = \langle r_{ij} | q \rangle \langle R_{ij} | P \rangle$$

$$+ \int d^3 r'_{ij} \langle r_{ij} | Q S_2(P) | r'_{ij} \rangle \langle r'_{ij} | q \rangle \langle R_{ij} | P \rangle$$

$$= [1 + g(r_{ij})] \langle r_{ij} | q \rangle \langle R_{ij} | P \rangle, \quad (\text{A7})$$

where q is the relative momentum and

$$\langle r_{ij} | Q S_2(P) | r'_{ij} \rangle = g(r_{ij}) \delta(r_{ij} - r'_{ij}). \quad (\text{A8})$$

Here the dependence on the total momentum of the defect function has been neglected. This result shows that, under the stated assumptions, the correlated wave function can be written as

$$\Psi(\{r_i\}) = A \Pi_{k_1 k_2} [1 + g(r_{ij})] \langle r_i | k_1 \rangle \langle r_j | k_2 \rangle, \quad (\text{A9})$$

which has the form of the variational wave function, if we identify the factor $1 + g$ with the correlation function $f(r)$ of the variational method. The defect function in the mixed representation F_B has then to be compared with $F_V(r) \langle r | q \rangle$, as discussed in the text. Both F_B and F_V can be expanded in partial waves and compared channel by channel.

-
- [1] M. Baldo and G. F. Burgio, *Rep. Prog. Phys.* **75**, 026301 (2012).
 [2] M. Baldo, in *Nuclear Methods and the Nuclear Equation of State*, International Review of Nuclear Physics, edited by M. Baldo, Vol. 8 (World Scientific, Singapore, 1999), p. 1.
 [3] J. Navarro, R. Guardiola, and I. Moliner, in *Introduction to Modern Methods of Quantum Many-Body Theory and Their*

Applications, Vol. 7, edited by A. Fabrocini, S. Fantoni, and E. Krotscheck (World Scientific, Singapore, 2002).

- [4] S. Fantoni and S. Rosati, *Nuovo Cimento A* **20**, 179 (1974).
 [5] V. R. Pandharipande and R. B. Wiringa, *Rev. Mod. Phys.* **51**, 821 (1979).

- [6] S. Fantoni and V. R. Pandharipande, *Phys. Rev. C* **37**, 1697 (1988).
- [7] R. B. Wiringa, V. Ficks, and A. Fabrocini, *Phys. Rev. C* **38**, 1010 (1988).
- [8] O. Benhar *et al.*, *Nucl. Phys. A* **550**, 2010 (1992).
- [9] S. Fantoni and A. Fabrocini, *Lect. Notes Phys.* **510**, 119 (1998).
- [10] A. Akmal, V. R. Pandharipande, and D. G. Ravenhall, *Phys. Rev. C* **58**, 1804 (1998).
- [11] F. Arias de Saavedra, C. Bisconti, G. Co', and A. Fabrocini, *Phys. Rep.* **450**, 1 (2007).
- [12] B. S. Pudliner, V. R. Pandharipande, J. Carlson, and R. B. Wiringa, *Phys. Rev. Lett.* **74**, 4396 (1995).
- [13] K. E. Schmidt and S. Fantoni, *Phys. Lett. B* **446**, 99 (1999).
- [14] S. C. Pieper and R. B. Wiringa, *Annu. Rev. Nucl. Part. Sci.* **51**, 53 (2001).
- [15] J. Carlson, J. Morales Jr., V. R. Pandharipande, and D. G. Ravenhall, *Phys. Rev. C* **68**, 025802 (2003).
- [16] A. Gezerlis and J. Carlson, *Phys. Rev. C* **81**, 025803 (2010).
- [17] G. Wlazlowski and P. Magierski, *Phys. Rev. C* **83**, 012801 (2011).
- [18] A. Ramos, A. Polls, and W. Dickhoff, *Nucl. Phys. A* **551**, 45 (1993).
- [19] T. Alm *et al.*, *Nucl. Phys. A* **551**, 45 (1993).
- [20] Y. Dewulf, W. H. Dickhoff, D. Van Neck, E. R. Stoddard, and M. Waroquier, *Phys. Rev. Lett.* **90**, 152501 (2003).
- [21] T. Frick and H. Mütter, *Phys. Rev. C* **68**, 034310 (2003).
- [22] H. Mütter and W. H. Dickhoff, *Phys. Rev. C* **72**, 054313 (2005).
- [23] I. Vidana and A. Polls, *Phys. Lett. B* **666**, 232 (2008).
- [24] A. Rios, A. Polls, A. Ramos, and H. Muther, *Phys. Rev. C* **74**, 054317 (2006).
- [25] A. Rios, A. Polls, and I. Vidana, *Phys. Rev. C* **79**, 025802 (2009).
- [26] O. Benhar and A. Fabrocini, *Phys. Rev. C* **62**, 034304 (2000).
- [27] M. Baldo, M. Borromeo and C. Ciofi degli Atti, *Nucl. Phys. A* **604**, 429 (1996).
- [28] M. Modarres and Y. Younesizadeh, *Phys. Rev. C* **85**, 054305 (2012).
- [29] M. Baldo and C. Maieron, *J. Phys. G* **34**, R1 (2007).
- [30] M. Modarres, *J. Phys. G* **19**, 1349 (1993).
- [31] M. Baldo and L. S. Ferreira, *Phys. Rev. C* **59**, 682 (1999).
- [32] H. R. Moshfegh and M. Modarres, *Nucl. Phys. A* **792**, 201 (2007).
- [33] M. Modarres and J. M. Irvine, *J. Phys. G* **5**, 511 (1979).
- [34] G. H. Bordbar and M. Modarres, *J. Phys. G* **23**, 1631 (1997); *Phys. Rev. C* **57**, 7119 (1998).
- [35] R. B. Wiringa, V. G. J. Stoks, and R. Schiavilla, *Phys. Rev. C* **51**, 38 (1995).
- [36] M. Modarres and H. R. Moshfegh, *Prog. Theor. Phys.* **112**, 21 (2004); H. R. Moshfegh and M. Modarres, *Nucl. Phys. A* **759**, 79 (2005).
- [37] H. R. Moshfegh and M. Modarres, *Nucl. Phys. A* **792**, 201 (2007).
- [38] M. Modarres and H. R. Moshfegh, *Phys. Rev. C* **62**, 044308 (2000).
- [39] M. Modarres and H. R. Moshfegh, *Physica A* **388**, 3297 (2009).
- [40] M. Modarres, H. R. Moshfegh, and A. Sepahvand, *Eur. Phys. J. B* **31**, 159 (2003).
- [41] H. R. Moshfegh and S. Zaryouni, *Eur. Phys. J. A* **43**, 283 (2010); **45**, 69 (2010).
- [42] B. Friedman and V. R. Pandharipande, *Nucl. Phys. A* **361**, 502 (1981).
- [43] M. Modarres, A. Rajabi, and H. R. Moshfegh, *Phys. Rev. C* **76**, 064311 (2007).
- [44] M. Baldo and C. Maieron, *J. Phys. G: Nucl. Part. Phys.* **34**, R1 (2007).
- [45] H. Kümmel, H. K. Lührmann, and J. G. Zabolitzky, *Phys. Rep.* **36**, 1 (1978).
- [46] Jochen H. Heisenberg and Bogdan Mihaila, *Phys. Rev. C* **59**, 1440 (1999).
- [47] B. D. Day, in *Brueckner–Bethe Calculations of Nuclear Matter*, Proceedings of the School E. Fermi, Varenna 1981, edited by A. Molinari (Editrice Compositori, Bologna, 1983), pp. 1–72.
- [48] R. B. Wiringa, *Phys. Rev. C* **38**, 2967 (1988).
- [49] H. Q. Song, M. Baldo, G. Giansiracusa, and U. Lombardo, *Phys. Rev. Lett.* **81**, 1584 (1998).
- [50] M. Baldo, G. Giansiracusa, U. Lombardo, and H. Q. Song, *Phys. Lett. B* **473**, 1 (2000).
- [51] P. Grange', A. Lejeune, M. Martzloff, and J. F. Mathiot, *Phys. Rev. C* **40**, 1040 (1989).
- [52] Z. H. Li, U. Lombardo, H. J. Schulze, W. Zuo, L. W. Chen, and H. R. Ma, *Phys. Rev. C* **74**, 047304 (2006).
- [53] Z. H. Li, U. Lombardo, H. J. Schulze, and W. Zuo, *Phys. Rev. C* **77**, 034316 (2008).
- [54] R. Machleidt, K. Holinde and Ch. Elster, *Phys. Rep.* **149**, 1 (1987).
- [55] R. Machleidt, *Adv. Nucl. Phys.* **19**, 189 (1989).
- [56] M. Baldo and A. B. Shaban, *Phys. Lett. B* **661**, 373 (2008).
- [57] V. Somá and P. Bozek, *Phys. Rev. C* **78**, 054003 (2008).
- [58] H. F. Zhang, U. Lombardo, and W. Zuo, *Phys. Rev. C* **82**, 015805 (2010).